RSC Advances

ROYAL SOCIETY OF CHEMISTRY

www.rsc.org/advances

The role of the CO adsorption on Pt monolayers supported on flat and stepped Au surfaces: A density functional investigation†

Polina Tereshchuk,[a] Rafael L. H. Freire[b] and Juarez L. F. Da Silva*[a]

Received Xth XXXXXXXXXX 2013, Accepted Xth XXXXXXXXX 2013
First published on the web Xth XXXXXXXXXX 200X
DOI: 10.1039/b000000x

Ultrathin metal films supported on transition-metal (TM) surfaces have been considered as promising catalyst systems due to the possibility to tune their chemical activity by controlling substrate strain, composition, and ligand effects, however, our atomistic understanding of the atomic structure of those systems is far from satisfactory. In this work, we will report a density functional theory investigation of the the atomic structure of Pt overlayer, skin of PtAu alloy, and Pt submonolayer on the Au(111) and Au(332) substrates, as well as the effects induced by CO adsorption. For uncovered CO surfaces, we found the same trend for both Au surfaces, i.e., there is a strong Pt preference for submonolayer sites, which is consistent with experimental findings and segregation energy calculations, however, the adsorption of CO molecules on the surfaces favors the location of the Pt atoms on the topmost surface layer due to the strong binding of CO molecules to the surface Pt atoms. For Pt/Au/Au(332), which is a high energy configuration, we found that the Pt overlayer adopts a Pt(111)-like structure instead of the expected Pt(332) overlayer following the Au(332) stacking, however, the steps are preserved once part of the Pt atoms are exchanged by Au atoms or CO molecules are adsorbed on the Pt overlayer, i.e., CO/Pt/Au/Au(332). Therefore, our results indicate that the atomic structure of Pt overlayer on flat and stepped Au surface under a CO atmosphere is complex due to the competing effects that favors different location for the Pt atoms, i.e., segregation energy and temperature effects favors subsurface sites, while strong CO−Pt binding energy favors the topmost surface layers.

1 Introduction

Ultrathin metal films composed of one or few layers supported on flat or stepped transition-metal (TM) surfaces have been considered as promising catalyst systems for several reactions due to the possibility to tune their chemical activity by controlling substrate strain, composition, and ligand effects.[1–3] TM layers supported on TM surfaces, such as (111), (100), and (110), have been widely studied, e.g., Fe, Co, Ni, and Pd on Au(111) and Au(110),[4–9] Co/Ag(111),[7] Co and PtAu on Pt(111),[10,11] Pt and Au on Ni(110),[12–14] Pt/Ni(111),[15] Pt and Au on Ru(0001),[16] Ag and Au on Cu(100),[17] Au/Cu(110),[18] Ag and Au on Pd(100),[17] and Au/Ir(111).[19] Among those systems, Pt layers supported on Au surfaces have attracted great interest, in particular, for the designing of high performance fuel cell electrocatalysts to improve oxygen reduction reactions.[20–23]

Scanning tunneling microscopy (STM) and temperature programmed desorption (TPD) studies have reported the formation of skin of PtAu alloys on Au(111) for Pt coverage of 3%, while Pt islands have been observed for higher Pt coverages at room temperature.[24] Electrochemistry experiments using cyclic voltammetry measurements have identified the formation of Pt monolayers on Au(111),[21,25] where the formation of the $(\sqrt{3}\times\sqrt{3})R30°$ and (1×1) Pt surface structures on Au(111) have been revealed.[21] Moreover, electrochemical experiments of the deposition of Pt atoms on Au vicinal surfaces, n(111)×(110), has demonstrated that Pt layer does not keep the structure of the Au(hkl) substrate.[26] Other experimental studies of the Pt/Au(111) system have revealed that Pt atoms are preferentially located in submonolayer sites.[3,22] Thus, those results indicate that the formation of well-defined Pt monolayer and skin PtAu alloys on Au surfaces depends strongly on the experimental conditions, in particular, on the Pt coverage, temperature, surface orientation, electrochemistry potentials, and etc.[3,21,22,24,25,27]

Several theoretical investigations have been performed to identify the atomic structures and chemical activity of Pt overlayer and skin of PtAu alloys on Au(111).[24,28–30] For example, it was reported that the formation of a skin of PtAu alloy is energetically more

[a] *Instituto de Química de São Carlos, Universidade de São Paulo, Caixa Postal 780, 13560-970, São Carlos, SP, Brazil; E-mail: juarez_dasilva@iqsc.usp.br*
[b] *Instituto de Fisica de São Carlos, Universidade de São Paulo, Caixa Postal 780, 13560-970, São Carlos, SP, Brazil*

favourable than a Pt overlayer supported on Au(111),[28] and hence, the chemical activity of the PtAu/Au(111) substrate is different from Pt(111) and Au(111), which was verified using the adsorption energy of CO molecules as a screening parameter.[30] It was found that CO binds stronger on pseudomorphic Pt overlayer on Au(111) than on Pt(111),[29] which was explained by the tensile strain present in the pseudomorphic Pt overlayer due to the large equilibrium lattice constant of bulk Au compared with bulk Pt.[31] Thus, the adsorption of CO molecules might play an important role on the formation of the PtAu skin on Au(111), as well as on the stability of the atomic structure of Pt overlayer on Au surfaces, in particular, due to the different magnitude of the CO adsorption energies on the Pt(111) and Au(111) surfaces, e.g., from −1.34 to −1.70 eV for CO/Pt(111) and from −0.12 to −0.32 eV for CO/Au(111).[32]

Thus, several studies have been reported on the formation of Pt overlayer and the skin of PtAu alloys on flat Au surfaces and the effects induced by the adsorption of CO molecules on the flat surfaces, however, our atomistic understanding of the structural effects induced by CO adsorption on Pt overlayer and skin of PtAu alloy on stepped Au surfaces is far from satisfactory due to the lack of studies, which compromise our understanding of model catalysts systems. To contribute to the solution of this problem, in this work, we performed a first-principles investigation of the structural effects induced by the CO adsorption on the Pt/Au/Au(111) and Pt/Au/Au(332) systems based on density functional theory (DFT) using different CO coverages. Our results indicate that the CO adsorption plays an important role in the formation of the skin of PtAu alloy on Au surfaces, as well as on the reconstruction of the stepped Au(332) surface.

2 Theoretical Approach and Computational Details

The description of CO adsorption on the Pt(111) surface by density functional theory (DFT) within local or semilocal exchange-correlation (*xc*) energy functionals has been in debate for a long time,[33–39] as plain DFT is unable to provide a correct description for the CO adsorption site preference on Pt(111), as well as on different TM surfaces.[32,38–41] For example, plain DFT yields hollow sites for CO/Pt(111), while experimental studies found the on-top sites for CO/Pt(111).[42–44] Recent DFT calculations employing the random phase approximation[38] obtained a correct description of the CO adsorption site preference (on-top) and the magnitude of the adsorption energy, e.g., −1.31 eV for CO/Pt(111) in the ($\sqrt{3}\times\sqrt{3}$) surface unit cell. However, those calculations are computationally demanding, in particular, for stepped surfaces using large surface unit cells.

Although plain DFT does not describe well the CO adsorption site preference, we would like to point out that plain DFT yields a quite good description of the magnitude of the CO adsorption energies on TM surfaces, which can explain the success of the *d*-band model based on a large number of plain DFT calculations for CO adsorption on several TM surfaces.[32,45] In this work, we focus on the effects of CO adsorption on Pt monolayer and a skin of PtAu alloys on flat and stepped Au surfaces, in which the description of the adsorption site preference does not play a crucial role due to the large magnitude of the relative total energy among different configurations.

Our calculations are based on spin-polarized DFT within the generalized gradient approximation[46] (GGA) employing the formulation proposed by Perdew, Burke, and Erzenholf[47] (PBE) for the *xc* energy functional. The all-electron projected augmented wave (PAW) method[48,49] as implemented in the Vienna *Ab Initio* Simulation Package[50,51] (VASP) was employed to solve the Kohn-Sham equations. For the total energy calculations a plane-wave cutoff energy of 400 eV was used for all calculations. The CO/Pt/Au(111) and CO/Pt/Au(332) systems were modeled using the repeated slab geometry separated by a vacuum region of 20 Å. For Au(111), we employed a (3×3) unit cell and 5 layers in the slab (45 atoms), while for Au(332), which is a stepped surface with 6 atoms in the (111) terraces, i.e., 6(111)×(11$\bar{1}$),[52] we employed a (2×1) surface unit cell with 27 layers in the slab (54 atoms). A large number of layers is required for Au(332) surface due to the small interlayer separation, i.e., $\frac{a_0}{\sqrt{3}}$ for Au(111) and $\frac{a_0}{\sqrt{88}}$ for Au(332).[52]

For all calculations, we relaxed all layers except those layers in the bottom of the slab, which were kept fixed in their relaxed clean surface positions. For the Brillouin zone integration, we employed a 4×4×1 and 6×2×1 **k**-point meshes for the Au(111) and Au(332) surfaces, respectively. For all optimizations of the atomic structure using the conjugated gradient as implemented in VASP, the equilibrium geometries were obtained when the atomic forces are smaller than 0.025 eV/Å on each atom, and a total energy convergence of 10^{-4} eV.

The PBE equilibrium lattice constants of the Pt and Au bulk in the face-centered cubic (fcc) structure are 3.98 and 4.16 Å, respectively, i.e., 1.53% and 1.96% larger than the experimental results,[31] which is expected as the PBE functional commonly overestimated the equilibrium lattice constants of bulk materials.[53,54] Thus, the Au lattice constant is 4.52% larger than for Pt, which might play

an important role for the structure of Pt overlayer on Au surfaces.

3 Results

3.1 Atomic structure of the Pt/Au/Au(111) and Pt/Au/Au(332) surfaces

To understand the role of supported Pt monolayers and submonolayer on the Au(111) and Au(332) surfaces, we selected several model systems, e.g., Pt/Au/Au(111), PtAu/PtAu/Au(111), Au/Pt/Au(111), Pt/Au/Au(332), PtAu/PtAu/Au(332), and Au/Pt/Au(332), which take into account overlayer, intermixed, and submonolayer configurations. For the intermixed model, in which Pt and Au atoms form a skin of PtAu alloy on Au surfaces, we considered the following configurations $Pt_{0.5}Au_{0.5}/Pt_{0.5}Au_{0.5}$/Au(332) and $Pt_{0.33}Au_{0.67}/Pt_{0.67}Au_{0.33}$/Au(111). The relative total energies per surface area for the lowest energy configurations are summarized in Table 1, and the lowest energy configurations are shown in Figures 1 and 2.

We found the same trend for both Pt/Au/Au(111) and Pt/Au/Au(332) systems, i.e., a strong preference of the Pt atoms for subsurface lattice sites, which is consistent with experimental findings.[3,22] We would like to point out that segregation energy calculations using DFT suggest that the formation of a skin of PtAu alloy on Au(111) is energetically preferable compared with Pt overlayer on Au(111),[28] which is consistent with our results. For example, the Pt/Au/Au(111) configuration is 36.20 meV/Å^2 higher in energy than the lowest atomic configuration, Au/Pt/Au(111), while it is 25.16 meV/Å^2 for Pt/Au/Au(332). Thus, there is a stronger preference of Pt atoms for subsurface sites in the flat surfaces than on stepped surfaces.

For Pt/Au/Au(332), we found a strong reconstruction of the stepped Au(332) surface, i.e., the Pt overlayer adopts a Pt(111)-like structure instead of the expected Pt(332) overlayer following the Au(332) stacking, which gives an energy gain of 0.13 eV per Pt atom. However, the steps are preserved for the case in which part of the Pt atoms in the overlayer is exchanged by Au atoms, and a skin of PtAu alloy is formed, which helps to lower the total energy of the system. Therefore, at low temperature experiments, in which the Pt atoms are unable to diffuse to the subsurface sites, our results indicate that chemical reactions might behave very similar on both Pt/Au/Au(111) and Pt/Au/Au(332) substrates, i.e., no effects from the steps would be observed. In fact, those results are confirmed by electrochemistry experiments reported recently,[26] which found that Pt atoms supported on Au vicinal surfaces, n(111)×(110), do not form a fully epitaxial layer.

3.2 CO adsorption effects on the Pt/Au/Au(111) and Pt/Au/Au(332) surfaces

To obtain an atomistic understanding of the role of CO adsorption on the atomic structure of the Pt/Au/Au(111) and Pt/Au/Au(332) systems, we performed total energy calculations for CO/Pt/Au/Au(111) and CO/Pt/Au/Au(332), employing CO coverages of Θ_{CO} = 0.33, and 0.56 monolayers (ML) for Pt/Au/Au/(111) and Θ_{CO} = 0.50 and 0.67 ML for Pt/Au/Au(332). For those calculations, CO molecules were adsorbed initially at the on-top, bridge, hollow sites, and on the combination of those sites, e.g., top+bridge+hollow. Along of the geometry optimization, we found that the CO molecules change their adsorption sites in a large number of configurations due to the different binding for CO on Pt and Au atoms, adsorption site preference, and the strong repulsion among the CO molecules for high CO coverages. The lowest energy configurations are shown in Figures 1 and 2, and their relative total energies per surface area, adsorption energies, and average C−TM bond lengths are summarized in Table 1.

Except for CO/Pt/Au/Au(332), for which the adsorption of CO molecules reverse the step reconstruction of the clean Pt/Au/Au(332) surface, the adsorption of CO molecules do not affect the substrate structure beyond the well-known adsorbate induced interlayer relaxation effect, e.g., contractions of about −1.43% (Δd_{12}) for Au/Pt/Au(111) changes to expansion of about +1.51% for CO/Au/Pt/Au(111). As mentioned, for CO/Pt/Au/Au(332), the Pt(332) overlayer is stabilized upon CO adsorption instead of the Pt(111)-like surface obtained for the clean Pt/Au/Au(332) surface. We found that the CO/Pt(332)/Au/Au(332) configuration is 254 meV lower in energy than the CO/Pt(111)/Au/Au(332) for Θ_{CO} = 0.50 ML.

For Θ_{CO} = 0.33 and 0.50 ML, the lowest energy configurations are the intermixed PtAu/PtAu layers on the Au(111) and Au(332) surfaces, respectively, i.e., a skin of PtAu alloy is exposed to the vacuum region. As expected, for the intermixed PtAu layer, CO binds preferentially on the Pt atoms instead of the Au atoms, which can be explained as follows. The average adsorption energy on Pt(111) and Au(111) for Θ_{CO} = 0.33 ML are −1.78 and −0.29 eV, respectively, which is in agreement with previous DFT results.[32] The C−TM distances are about 1.84 and 2.01 Å for CO adsorbed on on-top sites on Pt(111) and Au(111) surfaces, respectively, which is

Table 1 Relative total energy (E_{rel}) per surface area, adsorption energy per CO molecule and the averaged C−TM bond lengths. Here E_{rel} corresponds to the negative (positive) values for lower (higher) energy structures, and surface area is 67.869 Å^2 and 81.685 Å^2 for Au(111) and Au(332) surfaces, respectively, calculated as given in Ref. 52. The adsorption sites for the lowest energy configurations are indicated in Figures 1 and 2.

	E_{rel} (meV/Å^2)	E_{ad} (eV)	d_{C-TM} (Å)		E_{rel} (meV/Å^2)	E_{ad} (eV)	d_{C-TM} (Å)
Pt/Au/Au(111)	0.00			Pt/Au/Au(332)	0.00		
PtAu/PtAu/Au(111)	−17.61			PtAu/PtAu/Au(332)	−4.36		
Au/Pt/Au(111)	−36.20			Au/Pt/Au(332)	−25.16		
3CO/Pt/Au/Au(111)	0.00	−1.96	2.05	6CO/Pt/Au/Au(332)	0.00	−1.57	2.06
3CO/PtAu/PtAu/Au(111)	−15.35	−1.91	1.85	6CO/PtAu/PtAu/Au(332)	−6.62	−1.60	1.89
3CO/Au/Pt/Au(111)	31.72	−0.43	2.14	6CO/Au/Pt/Au(332)	57.94	−0.44	2.00
5CO/Pt/Au/Au(111)	0.00	−1.72	2.08	8CO/Pt/Au/Au(332)	0.00	−1.43	2.06
5CO/PtAu/PtAu/Au(111)	19.55	−1.22	2.02	8CO/PtAu/PtAu/Au(332)	20.89	−1.17	2.08
5CO/Au/Pt/Au(111)	64.11	−0.36	1.99	8CO/Au/Pt/Au(332)	91.29	−0.24	2.07

consistent with a stronger CO binding to the Pt atoms. At higher CO coverages, i.e., Θ_{CO} = 0.56 and 0.67 ML, the lowest energy configurations are CO/Pt/Au/Au(111) and CO/Pt/Au/Au(332), respectively, which can be explained by the large number of CO molecules that preferentially bind to the Pt atoms.

Thus, our finding indicates that the atomic structure of the Pt/Au/Au(111) and Pt/Au/Au(332) substrate depend strongly on the CO coverage, and hence, the CO gas-pressure plays a crucial role. Furthermore, we would like to point that the relative total energy among the different CO adsorption sites are much smaller than the relative total energy among the different surface configurations, e.g., E_{rel} = 0.00, −15.35, and 31.72 meV/Å^2 for CO molecules on Pt/Au/Au(111), PtAu/PtAu/Au(111), and Au/Pt/Au(111), respectively, with Θ_{CO} = 0.33 ML, while E_{rel} = 0.00, 0.27, and 1.35 meV/Å^2 for the lowest, first and second energy isomers for Pt/Au/Au(111), respectively, with the same CO coverage. Therefore, the adsorption effects induced by CO on Pt/Au/Au(111) and Pt/Au/Au(332) do not depend on the adsorption site preference.

In the lowest energy structure, we found that CO molecules bind preferentially on a mixture of hollow and bridge sites on the Pt/Au/Au(111) and Pt/Au/Au(332) surfaces, which is similar to the results obtained for CO on the Pt(111) and Pt(332) surfaces for the same CO coverage. For PtAu/AuPt/Au(111) and PtAu/AuPt/Au(332), we found that CO molecules preferentially bind to the on-top Pt sites, which is expected as the CO binding energy is larger for CO/Pt(111) than for CO/Au(111), and on-top sites were also observed for CO/Au/Pt/Au(111) and CO/Au/Pt/Au(332) for Θ_{CO} = 0.33 and 0.50 ML. However, at higher CO coverages, Θ_{CO} = 0.56 and 0.67 ML, the lowest energy configurations are composed by the combination of top+bridge+hollow sites, which is due to the the large lateral repulsion interactions among the CO molecules. Our results are in good agreement with previous results.[29,30]

It can be seen in Table 1 that the average CO adsorption energies for 3CO/Pt/Au/Au(111) and 3CO/PtAu/AuPt/Au(111) have similar magnitude, i.e., −1.96 eV and −1.91 eV, respectively, which can be explained as follows. At low CO coverages, Θ_{CO} = 0.33 ML, all the CO molecules bind to the Pt atoms, and hence, there is no substantial difference between the Pt overlayer and a skin of PtAu alloy on Au(111). However, the same does not hold for Θ_{CO} = 0.56 ML due to the binding of CO molecules in adsorption sites with the sharing of Pt and Au atoms, which lowers the adsorption energy for CO on PtAu/AuPt/Au(111), e.g., −1.72 eV for 5CO/Pt/Au/Au(111) and −1.22 eV for 5CO/PtAu/AuPt/Au(111). The same trends can be seen for CO adsorption on the (332) substrates. We would like to point out that the reduction of the magnitude of the CO adsorption energy with increased CO coverages is due to the increased repulsive interactions among the CO molecules intermediate by the substrate.[55]

3.3 Density of states

To obtain a better understanding of the electronic structure properties, we calculated the total and local density of states (LDOS), which are shown in Figure 3. The LDOS were averaged for the atoms with the same chemical specie and different layers. The C and O peaks derived from C and O *s*-states are located in the regions of 24 − 25 eV and 10 eV below the Fermi level, while the C

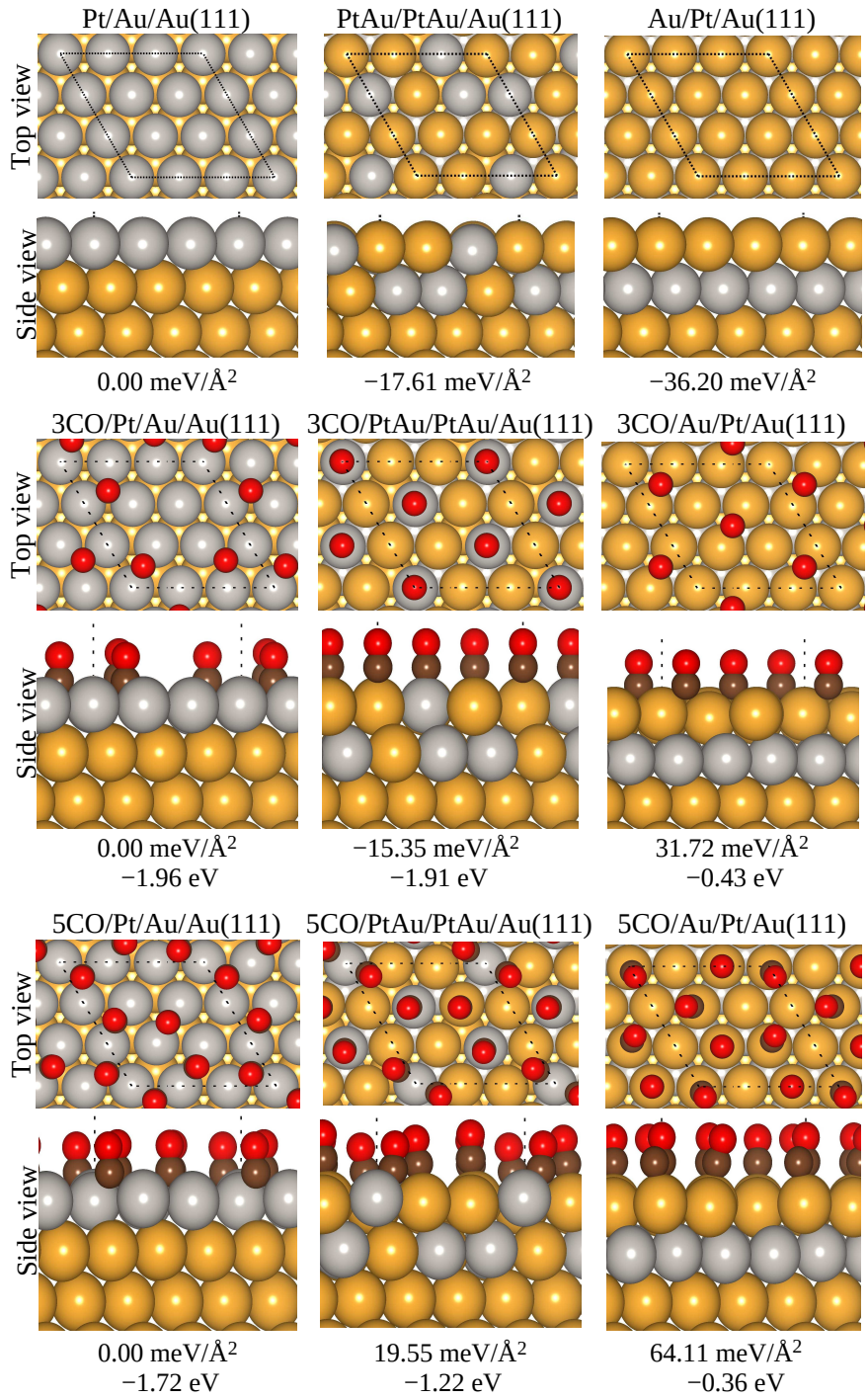

Fig. 1 Lowest energy configurations (top and side view) of the following systems, Pt/Au/Au(111), PtAu/PtAu/Au(111), Au/Pt/Au(111), CO/Pt/Au/Au(111), CO/PtAu/PtAu/Au(111), and CO/Au/Pt/Au(111), for Θ_{CO} = 0.33 and 0.56 ML, along with their relative total energies per surface unit area and average adsorption energies.

and O states derived from the p_x- and p_y-states spread in the region 6 – 8 eV below the Fermi level. The C and O p_z-states are located in the middle of the *d*-band, and a tail of the p_z-state extends above of the Fermi level denoting

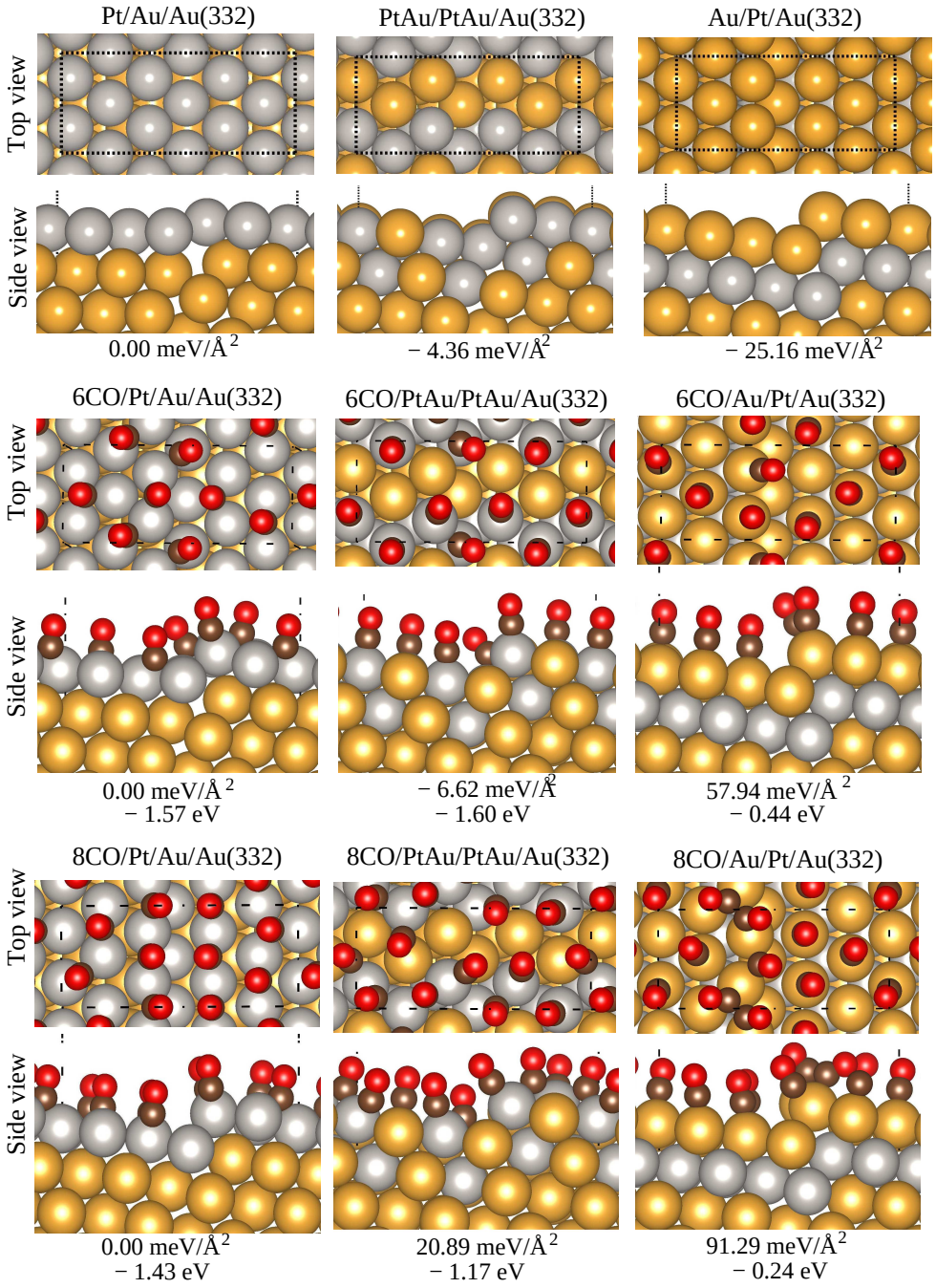

Fig. 2 Lowest energy configurations (top and side view) of the following systems, Pt/Au/Au(332), PtAu/PtAu/Au(332), Au/Pt/Au(332), CO/Pt/Au/Au(332), CO/PtAu/PtAu/Au(332), and CO/Au/Pt/Au(332), for Θ_{CO} = 0.50 and 0.67 ML, along with their relative total energies per surface unit area and average adsorption energies.

a depopulation of the C and O p_z-states. There is a small broadening of the C and O p_x- and p_y-states and larger broadening of the p_z-states, particularly for the C atoms, which indicates an overlap of the C p_z-orbitals with the Pt *d*-states. Moreover, there is a larger broadening of electronic states for CO adsorption on the (332) substrate compared with CO on (111), which can be explained by the higher CO coverage for CO on the (332) substrates.

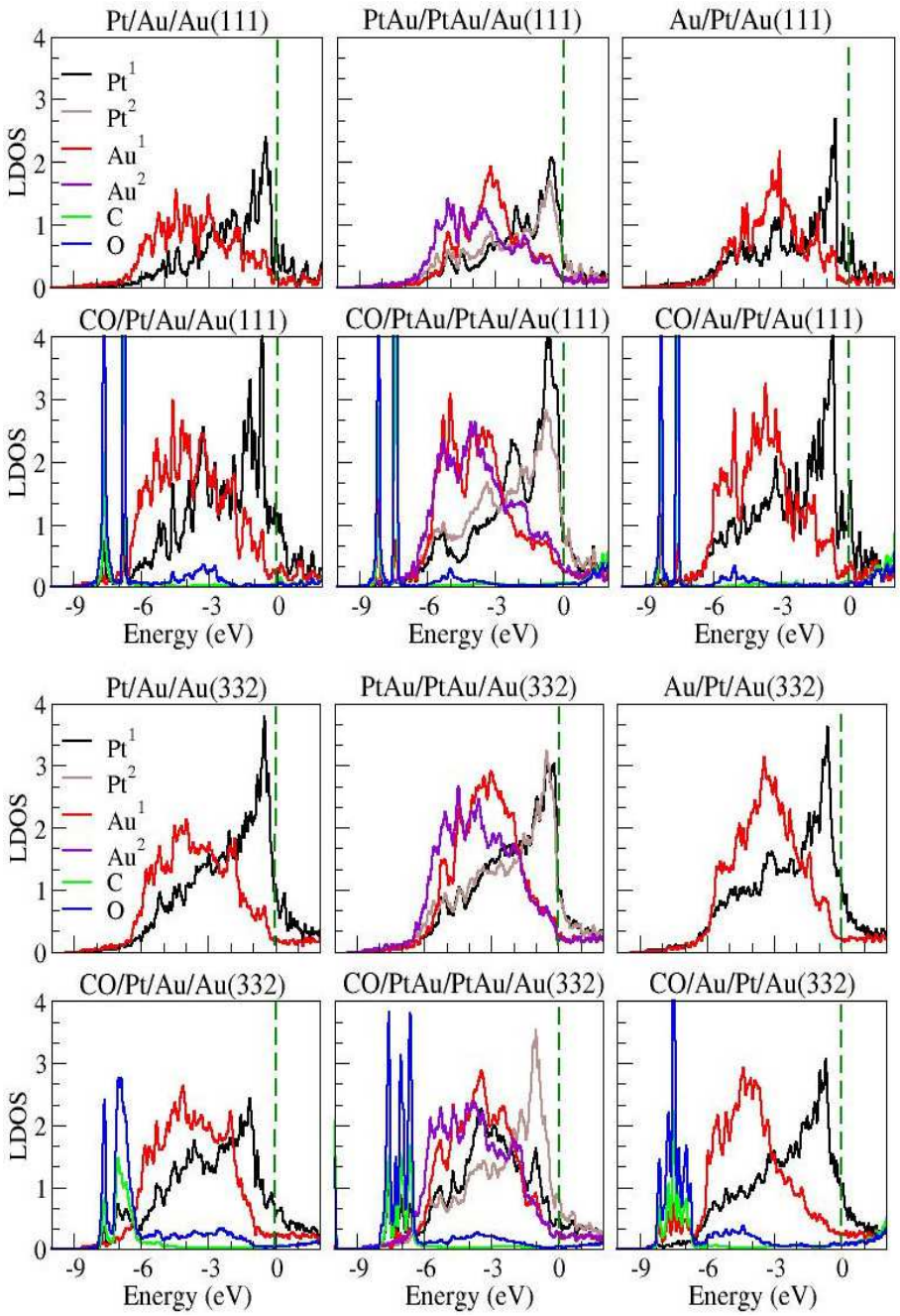

Fig. 3 Local density of states of the C, O, H, Pt and Au atoms for the lowest energy configurations of clean and CO adsorbed Pt/Au/Au(111), PtAu/PtAu/Au(111), Au/Pt/Au(111) and Pt/Au/Au(332), PtAu/PtAu/Au(332), Au/Pt/Au(332) with Θ_{CO} = 0.33 ML for (111) and 0.50 ML for (332) systems. The Pt^1, Pt^2, Au^1, and Au^2 indicates TM atoms of the first (1) and second (2) monolayers.

We calculated also the *d*-band center of the occupied *d*-states for the lowest energy configurations, which helps to understand the effect of Pt overlayer and the changes in the CO adsorption energies. As expected, our analysis of the LDOS show that the *d*-band center (occupied states) of the Pt atoms in the top most layer of the PtAu/PtAu/Au(111), PtAu/PtAu/Au(332), Pt/Au/Au(111), and Pt/Au/Au(332) systems is closer to

the Fermi level than for the Au(111) and Au(332) surfaces, and hence, based on the *d*-band model, we expect stronger CO adsorption energies, which is in fact observed in our calculations. We found that the adsorption of CO molecules on the substrates shifts the *d*-band center far from the Fermi level for the TM atoms binded directly to the CO molecule, which can be explained by the electron density transfer between the CO and substrate, i.e., the *d*-states are affected by the interaction. The shift is larger for CO binded on Pt atoms, which is expected due to the magnitude of the adsorption energies. For example, it is −1.79 eV for CO PtAu/PtAu/Au(111) at Θ_{CO} = 0.33 ML, however, the shift is smaller for different systems, i.e., −0.66 eV for 3CO/Pt/Au/Au(111).

4 Conclusion and Discussion

In this work, we report a first-principles density functional theory investigation of the atomic structure of Pt overlayer, skin of PtAu alloy, and Pt submonolayer on the Au(111) and Au(332) substrates, as well as the effects induced by CO adsorption on those systems using different CO coverages. We found the same trend for both substrates, i.e., there is a strong Pt preference for submonolayer sites, which is consistent with experimental findings[3,22] and segregation energy calculations.[28] Our results indicate a stronger Pt preference for submonolayer sites in flat surfaces than on stepped surfaces, which can be explained by differences in the release of strain energy. For Pt/Au/Au(332), which is not the lowest energy configuration but with great importance due to the initial steps for the formation of skin overlayer on Au surfaces, we found a strong reconstruction of the Pt overlayer, i.e., the Pt overlayer adopts a Pt(111)-like structure instead of the expected Pt(332) overlayer following the Au(332) stacking. However, the steps are preserved for the case in which part of the Pt atoms in the Pt overlayer are exchanged by Au atoms and a skin of PtAu alloy is formed on the Au(332) surface, and the lowest energy configuration is obtained once all the Pt atoms are exchanged by Au atoms.

Although our results indicate a strong preference of Pt atoms for subsurface sites in the flat and stepped Au surfaces, we would like to point out that those calculations are end-point configurations, i.e., highest energy Pt/Au/Au(332) and lowest energy Au/Pt/Au(332) configuration. Those configurations are separated by an energy barrier, i.e., the optimization of an initial configuration with Pt atoms on the surface, such as Pt/Au/Au(111) or Pt/Au/Au(332), does not lead to a new configuration with subsurface Pt atoms, as Au/Pt/Au(111) or Au/Pt/Au(332). Thus, temperature effects are expected to play a crucial role in the location of the Pt atoms on Au substrates. For example, at room temperature, scanning tunneling microscopy and temperature programmed desorption have obtained that the deposition of a 2.5 ML of Pt on Au(111) leads to the formation of a skin of PtAu alloy on Au(111),[24] i.e., not every Pt atom is located in subsurface sites. Thus, the segregation energy and temperature effects favors subsurface sites for Pt atoms on Au surfaces.

We found that the adsorption of CO molecules on those substrates play a crucial role in their atomic structure. For lower CO coverages, i.e., Θ_{CO} = 0.33 for Au(111) and 0.50 ML for Au(332), the lowest energy surface configurations is terminated by a skin of PtAu alloy on both Au(111) and Au(332) surfaces, and an increasing in the CO coverage decreases the number of subsurface Pt atoms, and for very high CO coverages, all the Pt atoms are located on the surfaces. For example, for Θ_{CO} = 0.56 ML for Au(111) and 0.67 ML for Au(332), the lowest energy configurations are CO/Pt/Au/Au(111) and CO/Pt/Au/Au(332). The presence of Pt atoms on the topmost surface layers can be explained as follows. The adsorption energy of CO molecules on Pt(111) is about six times larger than on the Au(111), e.g., the average adsorption energy on Pt(111) and Au(111) for Θ_{CO} = 0.33 ML are −1.78 and −0.29 eV, respectively. Thus, the CO adsorption on Pt overlayer favors the location of the Pt atoms on the topmost surface layer due to the strong binding energy of CO with Pt atoms.

Therefore, our results indicate clearly that the atomic structure of Pt overlayer on flat and stepped Au surface under a CO atmosphere is complex due to the competing effects that favors different location for the Pt atoms, i.e., segregation energy and temperature effects favors subsurface sites, while strong CO−Pt binding energy favors the topmost surface layers. Thus, our results and analysis indicate that experimental conditions play a crucial role in the atomic structure of Pt overlayer on flat and stepped Au surfaces.

5 Acknowledgments

Authors thank the São Paulo Research Foundation (FAPESP) and CAPES for the financial support and the infrastructure of the Centro de Informática de São Carlos, Universidade de São Paulo, for hosting our computer cluster.

References

1 R. R. Adzic, J. Zhang, K. Sasaki, M. B. Vukmirovic, M. Shao, J. X. Wang, A. U. Nilekar, M. Mavrikakis, J. A. Valerio and F. Uribe, *Top*

Catal., 2007, **46**, 249–262.
2 T. Bligaard and J. K. Nørskov, *Eletr. Acta*, 2007, **52**, 5512–5516.
3 S.-E. Bae, D. Gokcen, P. Liu, P. Mohammadi and S. R. Brankovic, *Electrocatal.*, 2012, **3**, 203–210.
4 J. A. Meyer, I. D. Baikie, E. Kopatzki and R. J. Behm, *Surf. Sci.*, 1996, **365**, L647–L651.
5 M. Kleinert, H.-F. Waibel, G. E. Engelmann, H. Martin and D. M. Kolb, *Electrochimica Acta*, 2001, **46**, 3129–3136.
6 F. Maroun, F. Ozanam, O. M. Magnussen and R. J. Behm, *Science*, 2001, **293**, 1811–1814.
7 K. Morgenstern, J. Kibsgaard, J. V. Lauritsen, E. Lægsgaard and F. Besenbacher, *Surf. Sci.*, 2007, **601**, 1967–1972.
8 T. Allmers and M. Donath, *New Journal of Physics*, 2009, **11**, 103049.
9 A. E. Baber, H. L. Tierney and E. C. H. Sykes, *ACS Nano*, 2010, **4**, 1637–1645.
10 C. S. Shern, S. L. Chen, J. S. Tsay and R. H. Chen, *Phys. Rev. B*, 1998, **58**, 7328–7332.
11 M. Eyrich, T. Diemant, H. Hartmann, J. Bansmann and R. J. Behm, *J. Phys. Chem. C*, 2012, **116**, 11154–11165.
12 L. P. Nielsen, F. Besenbacher, I. Stensgaard and E. Lagsgaard, *Phys. Rev. Lett.*, 1995, **74**, 1159–1162.
13 L. Porte, M. Phaner-Goutorbe, J. M. Guigner and J. C. Bertolini, *Surf. Sci.*, 1999, **424**, 262–270.
14 J.-S. Filhol, D. Simon and P. Sautet, *J. Am. Chem. Soc.*, 2004, **126**, 3228–3233.
15 J.-C. Bertolini, *Appl. Catal., A: Gen.*, 2000, **191**, 15–21.
16 A. Steltenpohl, N. Memmel, E. Taglauer, T. Fauster and J. Onsgaard, *Surf. Sci.*, 1997, **382**, 300–309.
17 P. w. Palmberg and T. N. Rhodin, *J. Chem. Phys.*, 1968, **49**, 134–146.
18 G. Kyriakou, F. J. Williams, M. S. Tikhov, A. Wander and R. M. Lambert, *Phys. Rev. B*, 2005, **72**, 121408.
19 M. Okada, M. Nakamura, K. Moritani and T. Kasai, *Surf. Sci.*, 2003, **523**, 218–230.
20 M. F. Mrozek, Y. Xie and M. J. Weaver, *Anal. Chem.*, 2001, **73**, 5953–5960.
21 J. Kim, C. Jung, C. K. Rhee and T. Lim, *Langmuir*, 2007, **23**, 10831–10836.
22 N. Kristian, Y. Yan and X. Wang, *Chem. Commun.*, 2008, 353–355.
23 A. Sarapuu, S. Kallip, A. Kasikov, L. Matisen and K. Tammeveski, *Journal of electroanalytical chemistry*, 2008, **624**, 144–150.
24 M. Ø. Pedersen, S. Helveg, A. Ruban, I. Stensgaard, E. Lagsgaard, J. K. Nørskov and F. Besenbacher, *Surf. Sci.*, 1999, **426**, 395–409.
25 I. Bakos, S. Szabó and T. Pajkossy, *J. Solid State Electrochem*, 2011, **15**, 2453–2459.
26 M. J. Prieto and G. Tremiliosi-Filho, *Phys. Chem. Chem. Phys.*, 2013, **15**, 13184–13189.
27 V. Petkov, B. N. Wanjala, R. Loukrakpam, J. Luo, L. Yang, C.-J. Zhong and S. Shastri, *Nano Lett.*, 2012, **12**, 4289–4299.
28 A. Christensen, A. V. Ruban, P. Stoltze, K. W. Jacobsen, H. L. S. J. K. Nørskov and F. Besenbacher, *Phys. Rev. B*, 1997, **56**, 5822–5834.
29 Y. Gohda and A. Gross, *Journal of Electroanalytical Chemistry*, 2007, **607**, 47–53.
30 Y. Gohda and A. Gross, *Surf. Sci.*, 2007, **601**, 3702–3706.
31 C. Kittel, *Introduction to Solid State Physics,* 7th ed., John Wiley & Sons, New York, 1996.
32 M. Gajdoš, A. Eichler and J. Hafner, *J. Phys.: Condens. Matter*, 2004, **16**, 1141.
33 B. Hammer, O. H. Nielsen and J. K. Nørskov, *Catal. Lett.*, 1997, **46**, 31–35.
34 P. J. Feibelman, B. Hammer, Nørskov, F. Wagner, M. Scheffler, R. Stumpf, R. Watwe, and J. Dumesic, *J. Phys. Chem. B*, 2001, **105**, 4018–4025.
35 A. Gil, A. Clotet, J. M. Ricart, G. Kresse, M. Garcia-Hernandez, N. Rosch and P. Sautet, *Surf. Sci.*, 2003, **530**, 71.
36 G. Kresse, A. Gil and P. Sautet, *Phys. Rev. B*, 2003, **68**, 073401.
37 M. Alaei, H. Akbarzadeh, H. Gholizadeh and S. de Gironcoli, *Phys. Rev. B*, 2008, **77**, 085414.
38 L. Schimka, J. Harl, A. Stroppa, A. Grüneis, M. Marsman, F. Mittendorfer and G. Kresse, *Nature Mater.*, 2010, **9**, 741–744.
39 P. Lazić, M. Alaei, N. Atodiresei, V. Caciuc, R. Brako and S. Blügel, *Phys. Rev. B*, 2010, **81**, 045401.
40 M. Neef and K. Doll, *Surf. Sci.*, 2006, **600**, 1085.
41 S. E. Mason, I. Grinberg and A. M. Rappe, *Phys. Rev. B*, 2004, **69**, 161401(R).
42 B. E. Hayden, K. Kretzschmar and A. M. Bradshaw, *Surf. Sci.*, 1985, **149**, 394–406.
43 D. Ogleterr, M. V. Hove and G. Somorjai, *Surf. Sci.*, 1986, **173**, 351–365.
44 G. S. Blackman, M.-L. Xu, D. F. Ogletree, M. A. V. Hove and G. A. Somorjai, *Phys. Rev. Lett.*, 1988, **61**, 2352–2355.
45 B. Hammer, Y. Morikawa and J. K. Nørskov, *Phys. Rev. Lett.*, 1996, **76**, 2141–2144.
46 J. P. Perdew, J. A. Chevary, S. H. Vosko, K. A. Jackson, M. R. Pederson, D. J. Singh and C. Fiolhais, *Phys. Rev. B*, 1992, **46**, 6671–6687.
47 J. P. Perdew, K. Burke and M. Ernzerhof, *Phys. Rev. Lett.*, 1996, **77**, 3865–3868.
48 P. E. Blöchl, *Phys. Rev. B*, 1994, **50**, 17953–17979.
49 G. Kresse and D. Joubert, *Phys. Rev. B*, 1999, **59**, 1758–1775.
50 G. Kresse and J. Hafner, *Phys. Rev. B*, 1993, **48**, 13115–13126.
51 G. Kresse and J. Furthmüller, *Phys. Rev. B*, 1996, **54**, 11169–11186.
52 J. L. F. Da Silva, C. Cyrille, K. Schroeder and S. Blügel, *Phys. Rev. B*, 2006, **73**, 125402.
53 J. L. F. Da Silva, C. Stampfl and M. Scheffler, *Surf. Sci.*, 2006, **600**, 703–715.
54 P. Haas, F. Tran, P. Blaha, K. Schwarz and R. Laskowski, *Phys. Rev. B*, 2009, **80**, 195109.
55 B. Shan, Y. Zhao, J. Hyun, N. Kapur, J. B. Nicholas and K. Cho, *J. Phys. Chem. C*, 2009, **113**, 6088–6092.